Research Article

Jun Pan*, Haijun Wang*, Guiyao Ke, and Feiyu Hu

Creation of single-wing Lorenz-like attractors *via* a ten-ninths-degree term

https://doi.org/10.1515/phys-2025-0165
received March 03, 2025; accepted May 08, 2025

Abstract: In light of the subtle connection between the strange attractors and the degree of dynamical systems, in this study, we propose a new simple asymmetric Lorenz-like system and report the finding of single-wing Lorenz-like attractors, which can also be created by the collapse of asymmetric singularly degenerate heteroclinic cycles. Moreover, we prove the existence of a single heteroclinic orbit to the origin and the nontrivial equilibrium point. Besides, numerical simulations also verify the theoretical analysis.

Keywords: heteroclinic orbit, generalization of the second part of Hilbert's 16th problem, Lyapunov function, single-wing attractor, asymmetric singularly degenerate heteroclinic cycle

1 Introduction

As early as 1990, Cox introduced an asymmetric perturbation of the Lorenz system and illustrated the transition to complicated dynamics in parameter-space, *i.e.*, the classic Lorenz system with a constant ε in its second equation, to meet the need of the scenario of the real-life laboratory setup [1]. Enlightened by this thought, Lü *et al.* proposed the controlled Lü and Chen system and performed a mirror operation to merge together two simple single-wing attractors to obtain the compound structure of the Lü attractor and Chen attractor [2,3]. Unfortunately, Liu *et al.* revisited the controlled Chen system and discovered the significant difference between the two aforementioned simple single-wing attractors and the Chen attractor, *i.e.*, Lyapunov exponents and Lyapunov dimensions [4]. Meanwhile, Miranda and Stone transformed the original Lorenz system into the proto-Lorenz system, interpreting the Lorenz system as a double covering of the proto-Lorenz system [5].

On the one hand, the controlled Lorenz, Chen, and Lü systems are potential candidates that can generate single-wing Lorenz-like attractors, due to the cause of a constant controller. On the other hand, if the constant controller ε is considered as the variables with power of zero, *i.e.*, εx^0, or εy^0, or εz^0, *etc.*, then the controlled Lorenz, Chen, and Lü systems also enrich the generalization of Hilbert's 16th problem [6–8]. This implies that the degree of polynomials in the model under study may have something to do with the geometric structure of attractors and repellers (as long as they exist), and not only to their number and mutual position.

Researchers have extensively investigated the relationship between polynomial degrees and complex dynamics, particularly in systems exhibiting Lorenz-like attractors and singular orbits. In 2007, replacing x_1 of the Lorenz system with $\phi_1(x_1) = ax_1(x_1 - 1)(x_1 - 2)$ and coining two two-scroll Lorenz attractors starting from the initial conditions (2.524, 1, 1) and (2.526, 1, 1), Chen and Zhang proposed an open problem: degrees of $\phi_i(x_i)$ control the number of the attractors of $\dot{\mathbf{x}} = \Phi(\phi_1(x_1), \phi_2(x_2), \phi_3(x_3))$, $i = 1, 2, 3$ [9]. In 2022, Wang *et al.* introduced $\sqrt[3]{x}$ into the Yang system's second and third equations, revealing many hidden attractors [10,11]. Later on, by introducing $\sqrt[5]{x}$, they performed the same operation and illustrated more Lorenz-like attractors [12], and demonstrated that similar substitutions could expand the parameter ranges for chaotic attractors (they may be transient chaos, self-excited or hidden ones) that coexist with the unstable origin and a pair of stable node-foci. In 2024, Ke *et al.* [13] changed $\sqrt[3]{x}$ back to x for the Lorenz-like system [11] and found more self-excited Lorenz-like attractors in contrast to the sub-quadratic

*** Corresponding author: Jun Pan,** Department of Big Data Science, School of Science, Zhejiang University of Science and Technology, Hangzhou, 310023, P.R. China, e-mail: panjun@zust.edu.cn
*** Corresponding author: Haijun Wang,** School of Electronic and Information Engineering (School of Big Data Science), Taizhou University, Taizhou, 318000, P.R. China, e-mail: 2021033@tzc.edu.cn
Guiyao Ke: School of Information, Zhejiang Guangsha Vocational and Technical University of Construction, Dongyang, Zhejiang, 322100, P.R. China, e-mail: guiyao.ke@zjgsdx.edu.cn
Feiyu Hu: College of Sustainability and Tourism, Ritsumeikan Asia Pacific University, Beppu, 874-8577, Japan, e-mail: hu-feiyu@apu.ac.jp

one [10]. By replacing x of the extended Lorenz system with $\sin(x)$, Wang *et al.* found conjoined Lorenz-like attractors [14]. By inserting x^2 to the Yang system's second equation, Wang *et al.* revealed asymmetric singularly degenerate heterocliniccycles (SDHC) with nearby asymmetric two-wing attractors [15]. However, substituting x^2 for x, Li and Wang obtained the modified cubic Lorenz-like system and did not observe SDHC and chaotic attractors [16]. By changing x to $\sqrt[3]{x^2}$, the new derived sub-quadratic Lorenz-like system has neither SDHC nor strange attractors [17]. Fortunately, the aforementioned Lorenz-like systems were proved to have a single/pair of heteroclinic orbits using different Lyapunov functions.

However, now the question is: how to create single-wing Lorenz-like attractors through changing the degrees of state variables, if they exist? To the best of our knowledge, scholars seldom consider this topic. More importantly, studying such a system may shed light on the research hotspot, *i.e.*, data-driven predictions of the chaotic system [18–21]. To achieve this target, by increasing the degree of the linear term cx of the Yang system to $\frac{10}{9}$, we achieve the following contributions:

(1) Creating single-wing Lorenz-like attractors by a ten-ninths-degree term.
(2) Explaining the formation of single-wing Lorenz-like attractors through collapses of asymmetric SDHC.
(3) Establishing the existence of a heteroclinic orbit connecting S_0 and S'.

This proposed quadratic Lorenz-like system aligns with the third principle of Sprott [22], representing the Lorenz-like analogue with only six terms. It addresses a critical gap in traditional Lorenz-like models by leveraging fractional-degree nonlinearity to generate asymmetric dynamics. Unlike controlled Lorenz/Chen systems, which rely on constant perturbations, our model uses a ten-ninths-degree term $\sqrt[9]{x^{10}}$ to create single-wing attractors, offering a novel paradigm for studying how algebraic structures shape attractor geometry, contributing to the generalization of Hilbert's 16th problem, where polynomial degree is shown to govern not only the number of attractors but also their topological complexities. Furthermore, the results obtained may provide insights into the fractional analogues that generate single-wing Lorenz-like attractors [23], the numerical algorithm [24], and model-free prediction of chaotic dynamics [25], *etc.*

The remainder of this work is structured as follows. Section 2 details the construction of the new simple asymmetric Lorenz-like system and reports the main results. Section 3 rigorously demonstrates the presence of a single heteroclinic orbit to S_0 and S' when $0 < 2a \le b$ and $c \ne 0$. At last, Section 4 concludes the study and explores prospective research directions, with a focus on investigating hidden single-wing Lorenz-like attractors.

2 New Lorenz-like system and key results

By comparing those Lorenz-like systems [10– 13,15–17] and systematic experimentation, this section first introduces the following new asymmetric Lorenz-like system:

$$\dot{x} = a(y - x), \quad \dot{y} = c\sqrt[9]{x^{10}} - xz, \quad \dot{z} = -bz + xy, \tag{2.1}$$

where $a \ne 0, b, c \in \mathbb{R}$, and summarizes the local dynamics in the following theorem.

Theorem 2.1.
(1) Table 1 *presents the equilibria of system* (2.1).
(2) Tables 2 *and* 3 *list the local behaviors of* S_0 *and* S_z, *where* $W^s_{\text{loc}}/W^c_{\text{loc}}/W^u_{\text{loc}}$ *denote the locally stable/center/unstable manifolds, as shown in the study by Kuzenetsov* [26].
(3) Table 4 *lists the local behaviors of* S', *where*

$$W = \{(a,b,c)|abc \ne 0\}, \quad W_1 = \Big\{(a,b,c) \in W|a + b > 0, \; ab + \left(1 - \tfrac{a}{9b}\right)\sqrt[17]{(bc)^{18}} > 0, \; \tfrac{17a\sqrt[17]{(bc)^{18}}}{9} > 0\Big\}, \quad W_2 = W\backslash W_1,$$

$$\triangle = ab(a+b) - \frac{(9ab - 9b^2 + a^2)\sqrt[17]{(bc)^{18}}}{9b},$$

Table 1: Equilibrium points

b	*c*	**Distribution of equilibria**
=0		$S_z = \{(0,0,z)|z \in \mathbb{R}\}$
≠0	=0	$S_0 = (0,0,0)$
	≠0	$S_0 = (0,0,0)$, $S' = \left(\sqrt[17]{(bc)^9}, \sqrt[17]{(bc)^9}, \frac{\sqrt[17]{(bc)^{18}}}{b}\right)$

Table 2: Local dynamics of S_0

b	*a*	*c*	**Property of S_0**
<0	<0		A 3D W^u_{loc}
	>0		A 1D W^s_{loc} and a 2D W^u_{loc}
>0	<0	=0	A 2D W^s_{loc} and a 1D W^u_{loc}
		≠0	A 1D W^s_{loc} and a 2D W^u_{loc}
	>0	=0	A 3D W^s_{loc}
		≠0	A 2D W^s_{loc} and a 1D W^u_{loc}

Table 3: Local dynamics of S_z

a	z	Property of S_z
<0	<0	A 1D W^c_{loc} and a 2D W^u_{loc}
	>0	A 1D W^s_{loc}, a 1D W^c_{loc} and a 1D W^u_{loc}
>0	<0	A 1D W^s_{loc}, a 1D W^c_{loc} and a 1D W^u_{loc}
	>0	A 2D W^s_{loc} and a 1D W^c_{loc}

Table 4: Local dynamics of S'

(a, c, b)	Property of S'
$W_1^1 \cup W_2$	Unstable
W_1^2	Hopf bifurcation
W_1^3	Asymptotically stable

$c_* = \frac{1}{b}\sqrt[18]{(\frac{9ab^2(a+b)}{9ab-9b^2+a^2})^{17}}$, $W_1^3 = \{(a,b,c) \in W_1 | \triangle > 0\}$, $W_1^2 = \{(a,b,c) \in W_1 | c = \pm c_*\}$, and $W_1^1 = \{(a,b,c) \in W_1 | \triangle < 0\}$.

Linear stability analysis for S_0 and S_z yields straightforward results, which are omitted here.

For S', the characteristic equation of the Jacobian matrix is calculated as

$$\lambda^3 + (a+b)\lambda^2 + \left[ab + \left(1 - \frac{a}{9b}\right)\sqrt[17]{(bc)^{18}}\right]\lambda + \frac{17a\sqrt[17]{(bc)^{18}}}{9} = 0, \tag{2.2}$$

from which, the local stability of S' is determined by the Routh–Hurwitz criterion. For $(a,b,c) \in W_1^2$, $\lambda_1 = -(a+b)$ and $\lambda_{2,3} = \pm\omega i = \pm\sqrt{\frac{17a^2b^2}{9ab-9b^2+a^2}}\, i$ are eigenvalues of S', *i.e.*, the roots of Eq. (2.2). Further, taking derivative on Eq. (2.2) with respect to c and replacing λ with ωi, one obtains $\frac{dRe(\lambda_2)}{dc}|_{c=\pm c_*} = \pm\frac{\sqrt[17]{bc_*}(9ab-9b^2+a^2)}{17[\omega^2+(a+b)^2]} \neq 0$ to verify the transversal condition, which leads to Hopf bifurcation at S', as shown in Figure 1. For the stability of Hopf bifurcation of S', the interested readers can apply the project method to determine it [26,27].

Second, based on Theorem 2.1 and using Matlab's procedure ode45 and Wolf Lyapunov exponent estimation [28], we delve more deeply into system (2.1) in the following single-wing Lorenz-like attractors and asymmetric SDHC.

For parameters $(a,b) = (5,1)$ and $(x_0^3, y_0^3, z_0^2) = (1.314, 1.618, 2.236)$, Figure 2 shows the bifurcation diagrams and Lyapunov exponents *vs* the parameter $c \in [-100, 100]$. Interestingly, the chaotic behaviors illustrated in Figure 1 display only single-wing Lorenz-like attractors rather than the two-wing ones, as shown in Figure 3.

Third, set $(a,c) = (0.5, \pm 6)$ and $(x_0^{4,5}, y_0^{4,5}) = (\pm 1.314, \pm 1.618) \times 10^{-7}$, $z_0^{3,4,5} = -1, -3, -5$, and $b \in [0,1]$. In order to detect asymmetric SDHC and their proximity to single-wing Lorenz-like attractors, we resort to the bifurcation diagrams and Lyapunov exponents *vs* the parameter c, as illustrated in Figures 4 and 5. Moreover, based on the dynamics of S_z listed in Table 3, we make a numerical study below.

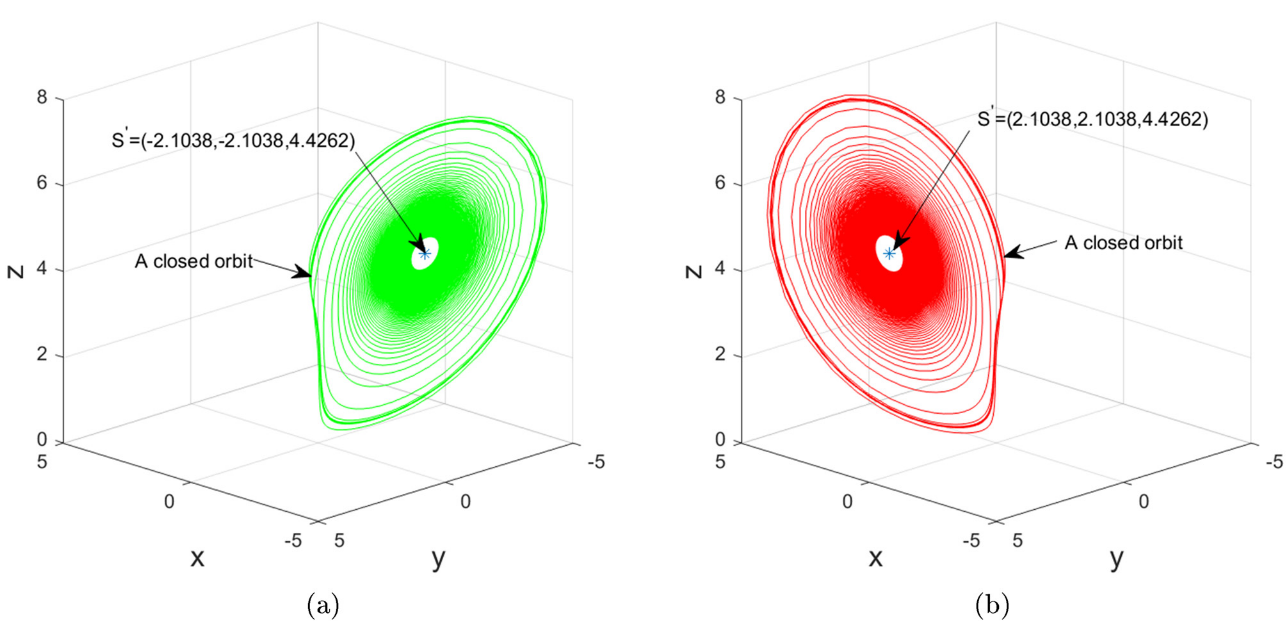

Figure 1: When $(a,b) = (5,1)$, (a) $c = -4.0751$, $(x_0^1, y_0^1, z_0^1) = (-2.323, -2.408, 4.429)$, (b) $c = 4.0751$, $(x_0^2, y_0^2, z_0^1) = (2.323, 2.408, 4.429)$, a closed orbit around S' when undergoing Hopf bifurcation. (a) $(a,c,b) = (5, -4.0751, 1)$ and (b) $(a,c,b) = (5, 4.0751, 1)$.

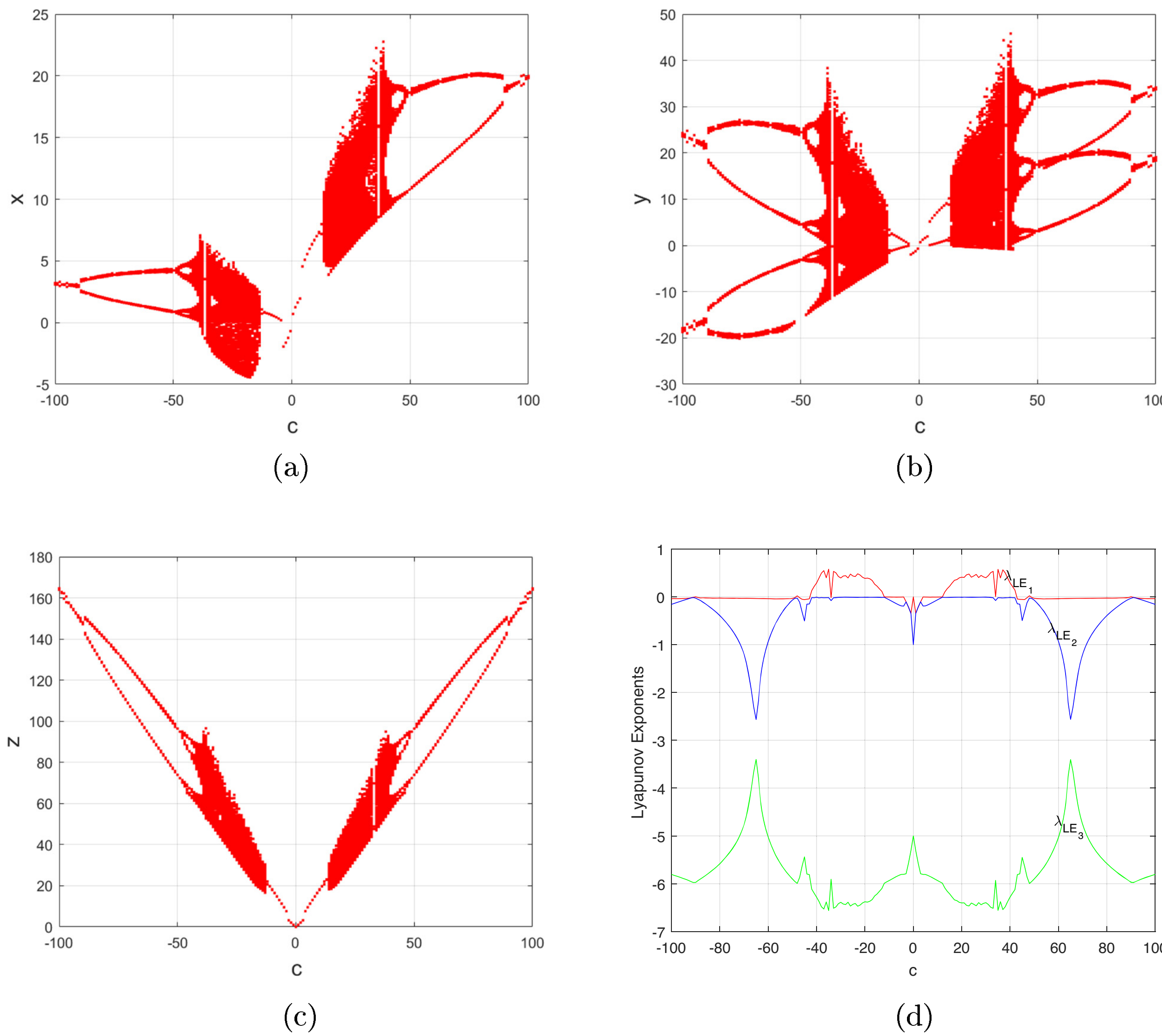

Figure 2: When $(a, b) = (5, 1)$ and $(x_0^3, y_0^3, z_0^2) = (1.314, 1.618, 2.236)$, (a), (b), (c) bifurcation diagrams and (d) Lyapunov exponents (λ_i, $i = 1, 2, 3$) *vs* the parameter c, yielding that system (2.1) experiences stable equilibrium point, Hopf bifurcation, period attractors, chaotic attractors when the parameter c varies. (a) $c -\ x$, (b) $c -\ y$, (c) $c -\ z$, and (d) Lyapunov exponents *vs* the parameter c.

Numerical Study 2.1 Set $c = 6$ (resp. -6), $a = 0.5$, $b = 0$, and $(x_0^4, y_0^4) = (1.314, 1.618) \times 10^{-7}$ (resp. $(x_0^5, y_0^5) = -(1.314, 1.618) \times 10^{-7}$), $z_0^{3,4,5} = -1, -3, -5$, Figure 6(a); resp. Figure 6(c) the one-dimensional unstable manifold $W^u(S_{z_{1,2,3}})$ ($S_{z_{1,2,3}} = (0, 0, -1), (0, 0, -3), (0, 0, -5)$) tends to the stable (0, 0, 11.9519), (0, 0, 13.4969), and (0, 0, 15.0369) when $t \to \infty$, generating asymmetric SDHC. When the parameter $b > 0$ is slightly perturbed, the collapse of these heteroclinic cycles creates a single-wing Lorenz-type attractor, as shown in Figure 6(b) (resp. Figure 6(d)).

Finally, using two appropriate Lyapunov functions and imitating the ones from previous literature [10–17, 29–38], we prove the following theorem in Section 3.

Theorem 2.2. *If* $b \geq 2a > 0$, $c \neq 0$, *then*

(a) *closed orbits are nonexistent in system* (2.1);

(b) *system* (2.1) *does not have any homoclinic orbits*;

(c) *a single heteroclinic orbit to* S_0 *and* S' *only exists in system* (2.1).

In order to enhance the readability of the proof of the Section 3, the following symbols are introduced:

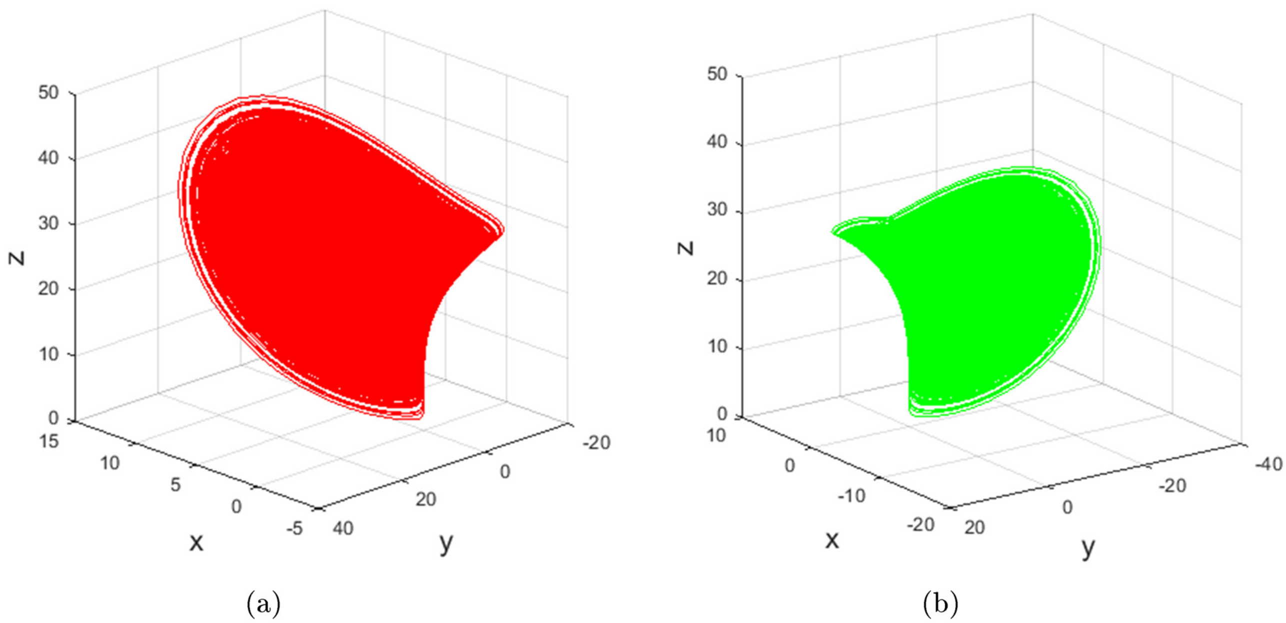

Figure 3: When $(a, b) = (5, 1)$ and $(x_0^3, y_0^3, z_0^2) = (1.314, 1.618, 2.236)$, (a) $c = 18$, (b) $c = -18$, single-wing Lorenz-like attractors depicted in Figure 2. (a) $c = 18$ and (b) $c = -18$.

(1) $\psi_t(p_0) = (x(t; x_0), y(t; y_0), z(t; z_0))$: every one orbit of system (2.1) originating from the initial condition $p_0 = (x_0, y_0, z_0)$.
(2) $W^u_{\mp}$: the negative and positive branches of the unstable manifold $W^u(S_0)$ corresponding to $x > 0$ and $x < 0$ as $t \to -\infty$.

3 Heteroclinic orbit

In this section, we first give the following two Lyapunov functions and the corresponding derivatives along $\psi_t(p_0)$
(1) $b - 2a > 0$

$$\begin{aligned} V_1(\psi_t(p_0)) = {} & b(b-2a)(y-x)^2 + (-bz + x^2)^2 \\ & + \frac{9(b-2a)}{19a}(-bc\sqrt[9]{x} + x^2)^2 \\ & + \frac{(b-2a)}{38a}(-\sqrt[17]{(bc)^{18}} + x^2)^2 \\ & + \frac{8(b-2a)\sqrt[17]{(bc)^{32}}}{19a}(-\sqrt[17]{(bc)^2} + \sqrt[9]{x^2})^2 \\ & + \frac{4(b-2a)\sqrt[17]{(bc)^{30}}}{19a}(-\sqrt[17]{(bc)^2}\sqrt[9]{x} + \sqrt[9]{x^3})^2 \\ & + \frac{2(b-2a)\sqrt[17]{(bc)^{26}}}{19a}(-\sqrt[17]{(bc)^4}\sqrt[9]{x} + \sqrt[9]{x^5})^2 \\ & + \frac{(b-2a)\sqrt[17]{(bc)^{18}}}{19a}(-\sqrt[17]{(bc)^8}\sqrt[9]{x} + x)^2, \end{aligned}$$

$$\left.\frac{\mathrm{d}V_1(\psi_t(p_0))}{\mathrm{d}t}\right|_{(2.1)} = 2ab(2a-b)(x-y)^2 - 2b(x^2 - bz)^2. \tag{3.1}$$

(2) $2a = b > 0$

$$\begin{aligned} V_2(\psi_t(p_0)) = {} & 38(y-x)^2 + 18(-2ac\sqrt[9]{x} + x^2)^2 \\ & + 16\sqrt[17]{(2ac)^{32}}(-\sqrt[17]{(2ac)^2} + \sqrt[9]{x^2})^2 \\ & + 8\sqrt[17]{(2ac)^{30}}(-\sqrt[17]{(2ac)^2}\sqrt[9]{x} + \sqrt[9]{x^3})^2 \\ & + 4\sqrt[17]{(2ac)^{26}}(-\sqrt[17]{(2ac)^4}\sqrt[9]{x} + \sqrt[9]{x^5})^2 \\ & + 2\sqrt[17]{(2ac)^{18}}(-\sqrt[17]{(bc)^8}\sqrt[9]{x} + x)^2 \\ & + (-\sqrt[17]{(2ac)^{18}} + x^2)^2, \end{aligned}$$

$$\left.\frac{\mathrm{d}V_2(\psi_t(p_0))}{\mathrm{d}t}\right|_{(2.1)} = -76a(x-y)^2. \tag{3.2}$$

Following the procedure in [10–17,29–39], one has to prove Lemma 3.1.

Lemma 3.1. *Suppose $c \neq 0$ and $0 < 2a \leq b$. The following statements hold.*
(i) If $\exists t_i, i = 1, 2,\ t_2 > t_1$, and $V_{1,2}(\psi_{t_1}(p_0)) = V_{1,2}(\psi_{t_2}(p_0))$, then $p_0 \in \{S_0, S'\}$.
(ii) If $\exists t \in \mathbb{R},\ x(t; x_0) > 0$ (resp. <0), and $\psi_t(p_0) \to S_0$ as $t \to -\infty$, then $\forall t \in \mathbb{R},\ V_{1,2}(S_0) > V_{1,2}(\psi_t(p_0))$, and $x(t; x_0) > 0$ (resp. <0). Namely, $p_0 \in W^u_+$ (resp. W^u_-).

Proof. (i) Based on the hypothesis of (i) and Eqs (3.1) and (3.2), the fact $\frac{\mathrm{d}V_{1,2}(\psi_t(p_0))}{\mathrm{d}t} = 0$ for all $t \in (t_1, t_2)$ yields

$$\dot{x}(t; x_0) \equiv \dot{z}(t; z_0) \equiv \dot{y}(t; y_0) \equiv 0, \tag{3.3}$$

i.e., $p_0 \in \{S_0, S'\}$. Precisely speaking, if $b = 2a > 0$, the hypothesis of (i) suggests $x^2 \equiv 2az$. In fact, $Q(\psi_t(p_0)) = x^2 - 2az$ with $\frac{\mathrm{d}Q(\psi_t(p_0))}{\mathrm{d}t}|_{(2.1)} = -2aQ(\psi_t(p_0))$ leads to

$$Q(\psi_t(p_0)) = Q(\psi_\tau(p_0))e^{-2a(t-\tau)} \quad \text{for all } \tau, t \in \mathbb{R}. \tag{3.4}$$

Since the boundedness of $\psi_\tau(p_0)$ as $\tau \to -\infty$, Eq. (3.4) yields $Q(\psi_t(p_0)) \equiv 0$, *i.e.*, $x^2 \equiv 2az$. When $0 < 2a < b$, we arrive at $\psi_t(p_0) \in \{x^2 - bz = 0\} \cap \{y - x = 0\}$ leads to $\dot{z}(t, z_0) \equiv \dot{x}(t, x_0) \equiv 0$, resulting in $x(t) = y(t) = x_0$ and thus, $\dot{y}(t, y_0) = 0$, $\forall t \in \mathbb{R}$.

(ii) First, we prove $V_{1,2}(S_0) > V_{1,2}(\psi_t(p_0))$, $\forall t \in \mathbb{R}$. Otherwise, $\exists t_0 \in \mathbb{R}$, $0 < V_{1,2}(S_0) \le V_{1,2}(\psi_{t_0}(p_0))$ holds. Based on the continuity of $V_{1,2}$ in t and $\psi_t(p_0) \to S_0$ as $t \to -\infty$, $\exists t_n \to -\infty$ and $n_{1,2} > 0$, $|V_{1,2}(\psi_{t_n}(p_0)) - V_{1,2}(S_0)| < \varepsilon_{1,2}$ is true, $\forall \varepsilon_{1,2} > 0$ and $n > \max\{n_1, n_2\}$. Due to $t_n \to -\infty$ and $t_0 \in \mathbb{R}$, $\exists n_{3,4}, t_0 > t_n$ holds, for all $\max\{n_{3,4}\} < n$. Set $n_0 = \max\{n_{1,2,3,4}\}$ and $\varepsilon_{1,2} = \frac{1}{2}[V_{1,2}(\psi_{t_0}(p_0)) - V_{1,2}(S_0)] \ge 0$. Then, $V_{1,2}(\psi_{t_n}(p_0)) - V_{1,2}(\psi_{t_0}(p_0)) = V_{1,2}(\psi_{t_n}(p_0)) - V_{1,2}(S_0) + V_{1,2}(S_0) - V_{1,2}(\psi_{t_0}(p_0)) < \varepsilon_{1,2} + V_{1,2}(S_0) - V_{1,2}(\psi_{t_0}(p_0)) = -\varepsilon_{1,2} \le 0$. Instead, the fact $\frac{\mathrm{d}V_{1,2}(\psi_t(p_0))}{\mathrm{d}t} \le 0$ in Eqs. (3.1) and (3.2) results in $V_{1,2}(\psi_{t_n}(p_0)) \ge V_{1,2}(\psi_{t_0}(p_0))$, $\forall t_n < t_0$, $n > n_0$. As a result, $V_{1,2}(\psi_{t_n}(p_0)) = V_{1,2}(\psi_{t_0}(p_0))$ and the hypothesis of (i) leads to $p_0 \in \{S_0, S'\}$. Because $\psi_t(p_0) \to S_0$, $p_0 \equiv S_0$, and $x(t, x_0) \equiv 0$ hold, $\forall t \in \mathbb{R}$, which yet conflict with the assumed condition that

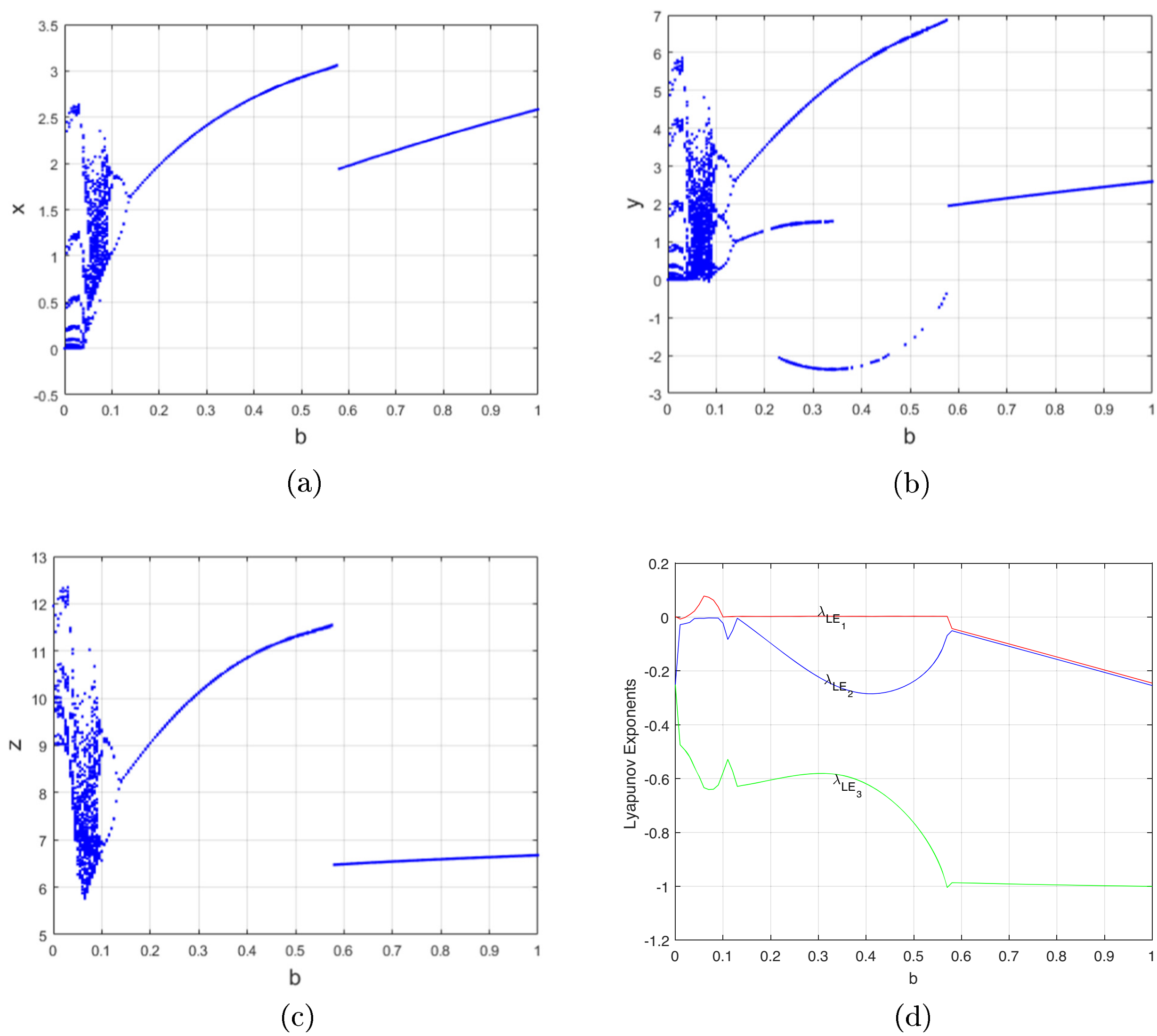

Figure 4: When $(a, c) = (0.5, 6)$ and $(x_0^4, y_0^4, z_0^3) = (1.314 \times 10^{-7}, 1.618 \times 10^{-7}, -1)$, (a), (b), (c) bifurcation diagrams and (d) Lyapunov exponents *vs* the parameter b, yielding the existence of SDHC with nearby bifurcated single-wing Lorenz-like attractors when the parameter $b > 0$ is slightly perturbed. (a) $b -\ x$, (b) $b -\ y$, (c) $b -\ z$, (d) Lyapunov exponents *vs* the parameter b.

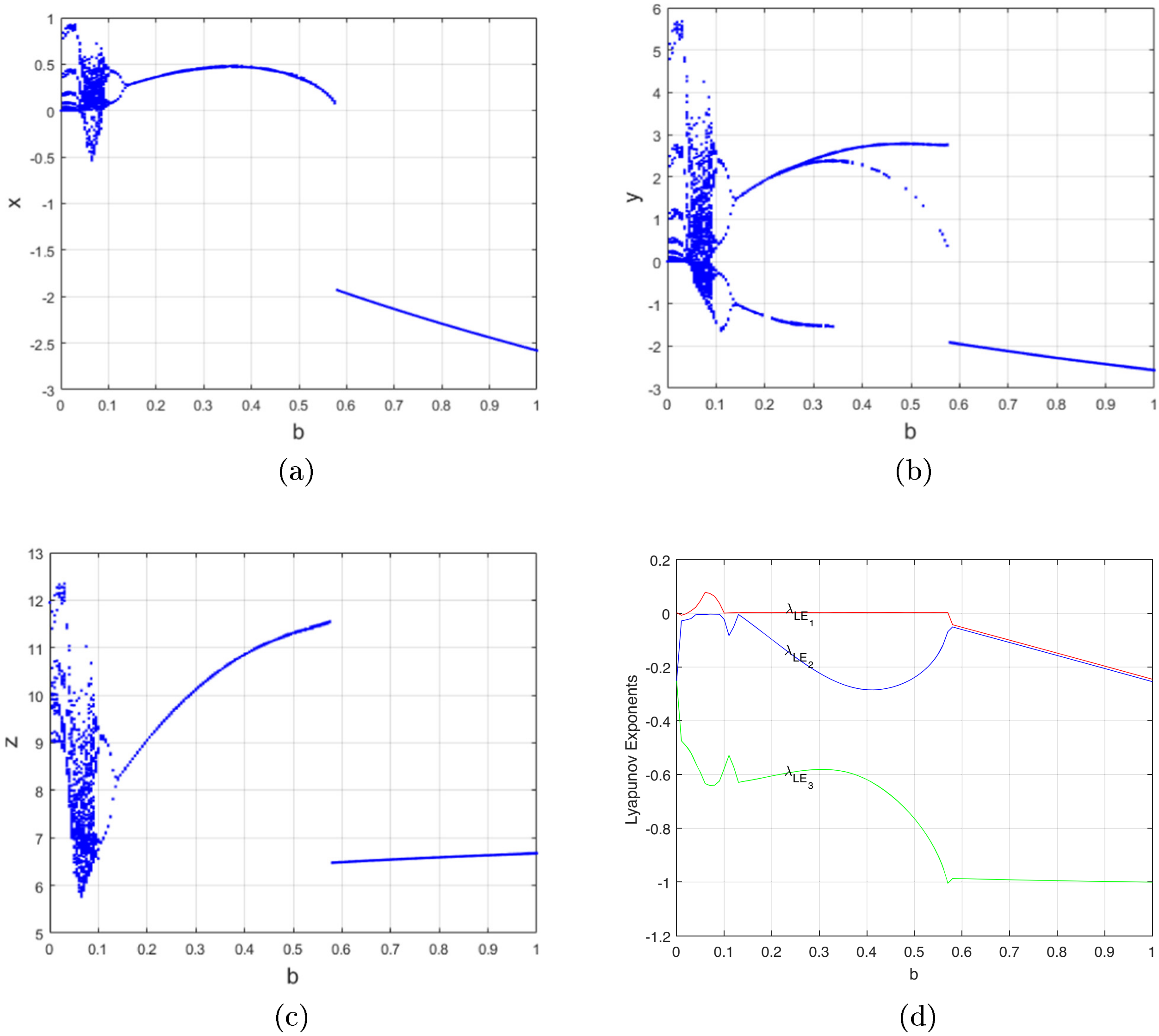

Figure 5: When $(a, c) = (0.5, -6)$ and $(x_0^5, y_0^5, z_0^3) = (-1.314 \times 10^{-7}, -1.618 \times 10^{-7}, -1)$, (a), (b), (c) bifurcation diagrams and (d) Lyapunov exponents *vs* the parameter b, yielding the existence of SDHC with nearby bifurcated single-wing Lorenz-like attractors when the parameter $b > 0$ is slightly perturbed. (a) $b - x$, (b) $b - y$, (c) $b - z$, (d) Lyapunov exponents *vs* the parameter c.

$x(t, x_0) > 0$ (resp. $x(t, x_0) < 0$), $\exists t \in \mathbb{R}$. Therefore, $V_{1,2}(S_0) > V_{1,2}(\psi_t(p_0))$, $\forall t \in \mathbb{R}$.

Further, we prove that $x(t, x_0) > 0$ (resp. $x(t, x_0) < 0$), for all $t \in \mathbb{R}$. Otherwise, there exists $t' \in \mathbb{R}$ such that $x(t', x_0) \le 0$ (resp. $x(t', x_0) \ge 0$) holds. On the other hand, $\exists t'' \in \mathbb{R}$, it follows from the hypothesis of (ii) that $x(t'', x_0) > 0$ (resp. $x(t'', x_0) < 0$) is also true. Therefore, $\exists \tau \in \mathbb{R}$, $x(\tau, x_0) = 0$ holds. Due to $V_{1,2}(\psi_t(p_0)) < V_{1,2}(S_0)$, $\forall t \in \mathbb{R}$, it follows that $\psi_\tau(p_0) \in \{\psi_t(p_0) | \; V_1(\psi_t(p_0)) < V_1(S_0)\} \cap \{\psi_t(p_0) | x = 0\} = \{\psi_t(p_0) | b(b-2a)y^2 + (bz)^2 + \frac{17(b-2a)\sqrt[17]{(bc)^{36}}}{38a} < \frac{17(b-2a)\sqrt[17]{(bc)^{36}}}{38a}\} = \varnothing$ for V_1, and $\psi_\tau(p_0) \in \{\psi_t(p_0) | 38x^2 + 17\sqrt[17]{(2ac)^{36}} < 17\sqrt[17]{(2ac)^{36}}\} = \varnothing$ for V_2, leading to a contradiction. As a result, $x(t, x_0) > 0$ (resp. $x(t, x_0) < 0$), $\forall t \in \mathbb{R}$. This completes the proof. □

Next the proof of Theorem 2.2 easily follows from Lemma 3.1.

Proof. (a) As $\frac{\mathrm{d}V_{1,2}(\psi_t(p_0))}{\mathrm{d}t} \le 0$ in Eqs (3.1) and (3.2) for $b \ge 2a > 0$, $c \ne 0$, we obtain

$$0 \le V_{1,2}(\psi_t(p_0)) \le V_{1,2}(p_0), \tag{3.5}$$

which suggests that $\lim_{t \to +\infty} V_{1,2}(\psi_t(p_0)) = V_{1,2}^*(p_0)$ exists. Namely, the boundedness of $V_{1,2}(\psi_t(p_0))$ also suggests that $\psi_t(p_0)$ is bounded for all $t \ge 0$. Let $\Omega(p_0)$ denote the ω-limit

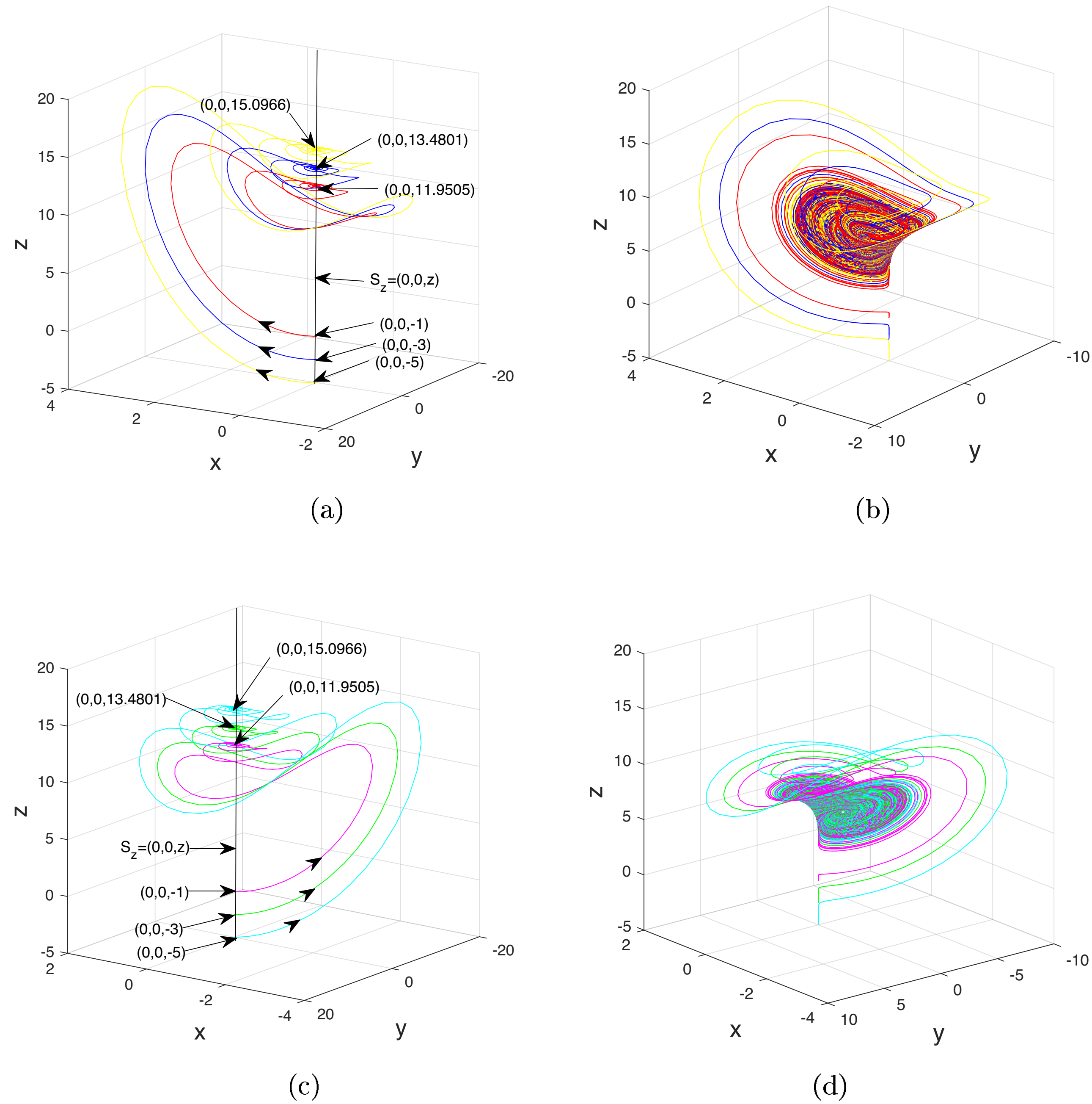

Figure 6: For $a = 0.5$, (a) $b = 0$, (b) $b = 0.06$, $(x_0^4, y_0^4) = (1.314, 1.618) \times 10^{-7}$, $z_0^{3,4,5} = -1, -3, -5$, (color in red, blue, and yellow), (c) $b = 0$, (d) $b = 0.06$, $(x_0^5, y_0^5) = -(1.314, 1.618) \times 10^{-7}$, $z_0^{3,4,5} = -1, -3, -5$ (color in magenta, green, and cyan), asymmetric SDHC with nearby single-wing Lorenz-like attractors suggested in Figures 4 and 5. (a) SDHC for $(a, c, b) = (0.5, 6, 0)$, (b) single-wing Lorenz-like attractor for $(a, c, b) = (0.5, 6, 0.06)$, (c) SDHC for $(a, c, b) = (0.5, -6, 0)$, and (d) single-wing Lorenz-like attractor for $(a, c, b) = (0.5, -6, 0.06)$.

set of the orbit $\psi_t(p_0)$. In a word, if $q \in \Omega(p_0)$, then every orbit through q belongs to $\Omega(p_0)$, *i.e.*, $\psi_t(p_0) \in \Omega(p_0)$. Consequently, $\forall \psi_t(q)$, $t \geq 0$, $\exists t_n \to \infty$ for $n \to \infty$, $\lim_{n \to +\infty} \psi_{t_n}(p_0) = \psi_t(q)$, leading to

$$V_{1,2}(\psi_t(q)) = \lim_{n \to +\infty} V_{1,2}(\psi_{t_n}(p_0)) = V_{1,2}^*(p_0) = \text{const},$$

$\forall t \geq 0$. Based on Lemma 3.1, $q \in \{S_0, S'\}$.

(b) Assume $\gamma(t, p_0)$ is a homoclinic orbit to S_0 or S', *i.e.*, $\lim_{t \to \pm\infty} \gamma(t, p_0) = o$, where $p_0 \notin \{S_0, S'\}$ and $o \in \{S_0, S'\}$. The fact $\frac{\mathrm{d}V_{1,2}(\psi_t(p_0))}{\mathrm{d}t} \leq 0$ in Eqs (3.1) and (3.2) leads to

$$\begin{aligned} 0 \leq V_{1,2}(o) = V_{1,2}(\gamma(-\infty, p_0)) &\leq V_{1,2}(\gamma(t, p_0)) \\ &\leq V_{1,2}(\gamma(\infty, p_0)) = V_{1,2}(o), \end{aligned}$$

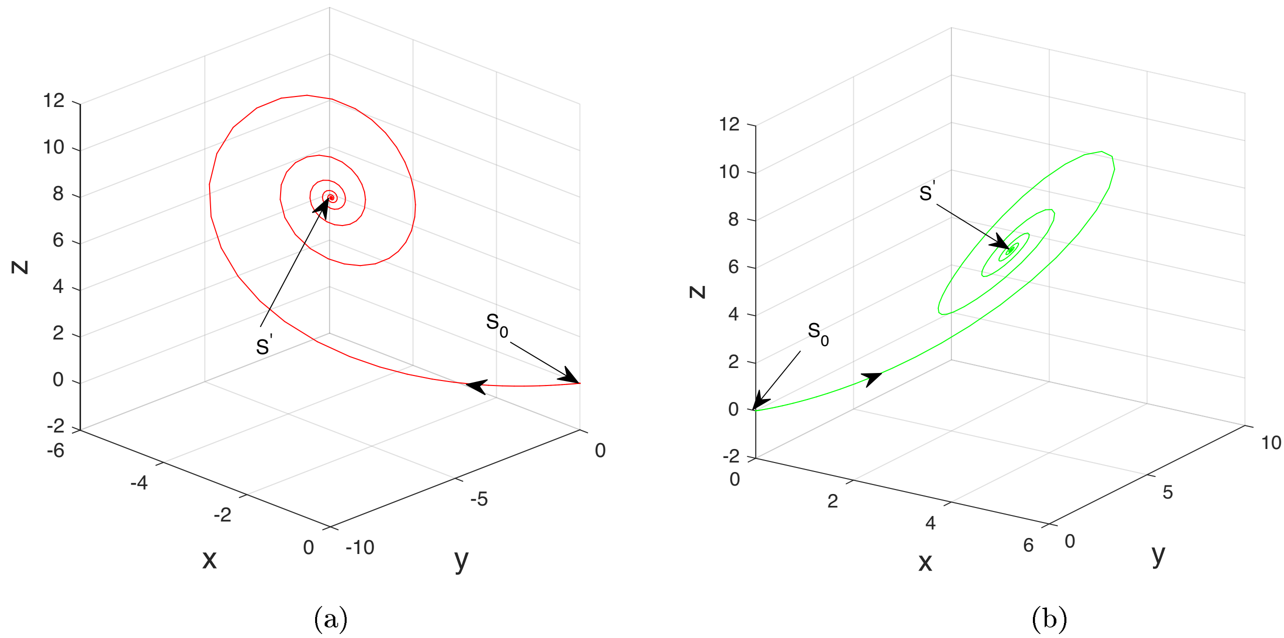

Figure 7: When $(a, b) = (1, 2)$, (a) $c = -6$, $(x_0^4, y_0^4, z_0^6) = (1.314, 1.618, 2.236) \times 10^{-7}$, (b) $c = 6$, $(x_0^5, y_0^5, z_0^6) = (-1.314, -1.618, 2.236) \times 10^{-7}$, an orbit heteroclinic to S_0 and S'. (a) $c = -6$ and (b) $c = 6$.

i.e. $V_{1,2}(\gamma(t, p_0)) = V_{1,2}(o)$, $\forall t \in \mathbb{R}$. According to Lemma 3.1(i), it follows that $p_0 \in \{S_0, S'\}$, resulting in a contradiction. Therefore, homoclinic orbits are non-existent in system (2.1).

(c) In light of (a), one-dimensional branch of $W_+^u(S_0)$ (resp. $W_-^u(S_0)$) has an ω-limit, *i.e.*, $q \in \{S_0, S'\}$. Since $V_{1,2}(S_0) > V_{1,2}(S')$, q must be S', resulting in the formation of one and only one heteroclinic orbit to S_0 and S', as shown in Figures 7 and 8. The proof is complete. □

4 Conclusion

In the sense of generalizing the second part of Hilbert's renowned 16th problem, this study replaces the linear term cx of the Yang system with the ten-ninths-degree term $c\sqrt[9]{x^{10}}$, and creates single-wing Lorenz-like attractors, asymmetric SDHC, single heteroclinic orbit, *etc*. Notably,

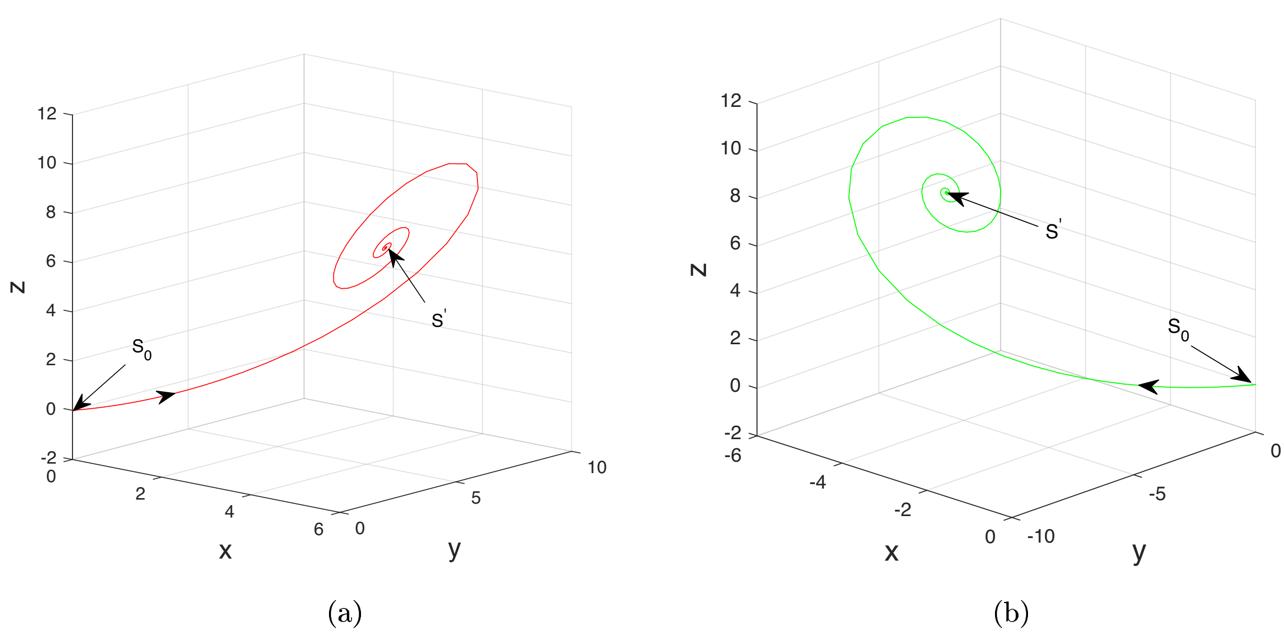

Figure 8: When $(a, b) = (1, 3)$, (a) $c = 6$, $(x_0^4, y_0^4, z_0^6) = (1.314, 1.618, 2.236) \times 10^{-7}$, (b) $c = -6$, $(x_0^5, y_0^5, z_0^6) = (-1.314, -1.618, 2.236) \times 10^{-7}$, an orbit heteroclinic to S_0 and S'. (a) $c = 6$ and (b) $c = -6$.

the formation of single-wing Lorenz-like attractors may result from the collapse of these asymmetric SDHC, and that system casts a mirror image of these dynamics from $-c$ to c.

Compared with the controlled Lorenz, Chen, and Lü systems with various strange attractors (*i.e.*, asymmetric two-wing ones, partial ones, and single-wing ones), the newly reported one only generates single-wing ones. To some extent, this exotic phenomenon contributes to the broader understanding of Hilbert's sixteenth problem, *i.e.*, the degree also makes a real impact on the geometrical structure of strange attractors, except for the number and mutual disposition [6,7,11–13].

However, it is unclear whether there are hidden single-wing Lorenz-like attractors in that studied system or not. In what follows, we will continue to uncover the correction between the degrees and strange attractors, and provide reference for real world applications. The asymmetric single-wing attractors proposed here have promising applications in secure communication, where their asymmetric dynamics can enhance signal encryption robustness against symmetric attacks. In neural networks, the single-wing structure could model asymmetric information processing in biological systems, such as directional signal transmission in neural circuits. For system identification, stitching the right and left images of single-wing Lorenz-like attractor with $\pm c$ together complicates the problem of discovering governing equations [18].

Funding information: This work was supported in part by Zhejiang Public Welfare Technology Application Research Project of China under Grant LGN21F020003, and in part National Natural Science Foundation of China under Grant 12001489. Furthermore, the authors sincerely thank the anonymous editors and reviewers for their meticulous reading and constructive feedback, which have significantly enhanced the quality of this manuscript.

Author contributions: All authors have accepted responsibility for the entire content of this manuscript and approved its submission.

Conflict of interest: The authors state no conflict of interest.

Data availability statement: All data generated or analyzed during this study are included in this published article.

References

[1] Cox SM. The transition to chaos in an asymmetric perturbation of the Lorenz system. Phys Lett A. 1990;144(6–7):325–8.

[2] Lü J, Chen G, Zhang S. The compound structure of a new chaotic attractor. Chaos Solitons Fractals. 2002;14(5):669–72.

[3] Lü J, Zhou T, Chen G, Zhang S. The compound structure of Chen's attractor. Int J Bifurcat Chaos. 2002;12(4):855–8.

[4] Liu J, Lu J, Wu X. Dynamical analysis for the compound structure of Chen's system. ICARCV 2004 8th Control, Automation, Robotics and Vision Conference, Kunming, China. Vol. 3. 2004. p. 2250–3.

[5] Miranda R, Stone E. The proto-Lorenz system. Phys Lett A. 1993;178:105–13.

[6] Leonov GA, Kuznetsov NV. On differences and similarities in the analysis of Lorenz, Chen, and Lu systems. Appl Math Comput. 2015;256:334–43.

[7] Kuznetsov NV, Mokaev TN, Kuznetsova OA, Kudryashova EV. The Lorenz system: hidden boundary of practical stability and the Lyapunov dimension. Nonlinear Dyn. 2020;102:713–32.

[8] Hilbert D. Mathematical problems. Bull. Am. Math. Soc. 1902;8:437–79.

[9] Zhang X, Chen G. Constructing an autonomous system with infinitely many chaotic attractors. Chaos Interdiscip J Nonlinear Sci. 2017;27(7):0711011–5.

[10] Liu Y, Yang Q. Dynamics of a new Lorenz-like chaotic system. Nonlinear Anal-Real. 2010;11(4):2563–72.

[11] Wang H, Ke G, Pan J, Hu F, Fan H. Multitudinous potential hidden Lorenz-like attractors coined. Eur Phys J Spec Top. 2022;231:359–68.

[12] Wang H, Pan J, Ke G. Revealing more hidden attractors from a new sub-quadratic Lorenz-like system of degree $\frac{6}{5}$. Int J Bifurcat Chaos. 2024;34(6):2450071–15.

[13] Ke G, Pan J, Hu F, Wang H. Dynamics of a new four-thirds-degree sub-quadratic Lorenz-like system. Axioms. 2024;13(9):625–16.

[14] Wang H, Ke G, Pan J, Su Q. Conjoined Lorenz-like attractors coined. Miskolc Mathematical Notes. 2023; code: MMN-4489, online, https://mat76.mat.uni-miskolc.hu/mnotes/forthcoming?volume=0&number=0#forthcoming.

[15] Wang H, Pan J, Hu F, Ke G. Asymmetric singularly degenerate heteroclinic cycles. Int J Bifurcat Chaos. 2025;35(6):2550072-1–14.

[16] Li X, Wang H. A three-dimensional nonlinear system with a single heteroclinic trajectory. J Appl Anal Comput. 2020;10(1):249–66.

[17] Wang H, Pan J, Ke G, Hu F. A pair of centro-symmetric heteroclinic orbits coined. Adv Cont Discr Mod. 2024;2024:1–11.

[18] Brunton SL, Proctor JL, Kutz JN. Discovering governing equations from data by sparse identification of nonlinear dynamical systems. PNAS. 2016;113(15):3932–7.

[19] Wan Z, Sapsis TP. Reduced-space Gaussian process regression for data-driven probabilistic forecast of chaotic dynamical systems. Phys D. 2017;345(15):40–55.

[20] Dubois P, Gomez T, Planckaert L, Perret L. Data-driven predictions of the Lorenz system. Phys D. 2020;408:132495-1–10.

[21] Karimov A, Rybin V, Kopets E, Karimov T, Nepomuceno E, Butusov D. Identifying empirical equations of chaotic circuit from data. Nonlinear Dyn. 2023;111:871–86.

[22] Sprott JC. A proposed standard for the publication of new chaotic systems. Int J Bifurcat Chaos. 2011;21(9):2391–4.

[23] Almutairi N, Saber S. Existence of chaos and the approximate solution of the Lorenz-Lü-Chen system with the Caputo fractional operator. AIP Advances. 2024;14:015112-1–16.

[24] Al-Raeei M, El-Daher MS. An algorithm for fractional Schrödinger equation in case of Morse potential. AIP Adv. 2020;10:035305-1–13.

[25] Tan H, Shi L, Wang S, Qu S. Improving model-free prediction of chaotic dynamics by purifying the incomplete input. AIP Adv. 2024;14:125225-1–10.
[26] Kuzenetsov YA. Elements of applied bifurcation theory. 3rd ed. New York: Springer-Verlag; 2004.
[27] Sotomayor J, Mello LF, Braga DC. Lyapunov coefficients for degenerate Hopf bifurcations. arXiv:0709.3949v1 [Preprint]. 2007 [cited 2007 Sep 25]: [16 p.]. https://arxiv.org/abs/0709.3949.
[28] Wolf A, Swift JB, Swinney HL, Vastano JA. Determining Lyapunov exponents from a time series. Phys D. 1985;16(3):285–317.
[29] Tigan G, Constantinescu D. Heteroclinic orbits in the T and the Lü system. Chaos Solitons Fractals. 2009;42(1):20–3.
[30] Chen Y, Yang Q. Dynamics of a hyperchaotic Lorenz-type system. Nonlinear Dyn. 2014;77(3):569–81.
[31] Wang H, Li C, Li X. New heteroclinic orbits coined. Int J Bifurcat Chaos. 2016;26(12):16501941–13.
[32] Wang H, Ke G, Pan J, Hu F, Fan H, Su Q. Two pairs of heteroclinic orbits coined in a new sub-quadratic Lorenz-like system. Eur Phys J B. 2023;96:1–9.
[33] Wang H, Ke G, Pan J, Su Q, Dong G, Fan H. Revealing the true and pseudo-singularly degenerate heteroclinic cycles. Indian J. Phys. 2023;976:3601–15.
[34] Wang H, Ke G, Pan J, Su Q. Modeling, dynamical analysis and numerical simulation of a new 3D cubic Lorenz-like system. Scientific Reports. 2023;13:6671–15.
[35] Li Z, Ke G, Wang H, Pan J, Hu F, Su Q. Complex dynamics of a sub-quadratic Lorenz-like system. Open Phys. 2023;21:20220251-1–15.
[36] Wang H, Ke G, Hu F, Pan J, Dong G, Chen G. Pseudo and true singularly degenerate heteroclinic cycles of a new 3D cubic Lorenz-like system. Results Phys. 2024;56:107243–13.
[37] Wang H, Pan J, Ke G. Multitudinous potential homoclinic and heteroclinic orbits seized. Electronic Res Archive. 2024;32(2):1003–16.
[38] Pan J, Wang H, Hu F. Revealing asymmetric homoclinic and heteroclinic orbits. Electronic Res Archive. 2025;33:1337–50.
[39] Pan J, Wang H, Hu F, Ke G. A novel Lorenz-like attractor and stability and equilibrium analysis. Axioms. 2025;14:264-1–17.